








Original Research Article

## Adsorption of Cd(II) onto Olive Stones Powder Biosorbent: Isotherms and Kinetic Studies

Khaled Muftah Elsherif<sup>1\*</sup>, Rima Abdessalem Abdullah Saad<sup>2</sup>, Abdunaser Mabrok Ewlad-Ahmed<sup>2</sup>, Abdullah Amhimmid Treban<sup>2</sup>, Abdulrhman Mohammed Iqneebir<sup>2</sup>

<sup>1</sup>Libyan Authority for Scientific Research, Tripoli, Libya

<sup>2</sup>Chemistry Department, Faculty of Arts and Science Msallata, ElMergib University, Al-Khoms, Libya

### ARTICLE INFO

#### Article history

Submitted: 11 September 2023

Revised: 08 October 2023

Accepted: 30 October 2023

Available online: 31 October 2023

Manuscript ID: [AJCA-2308-1415](#)

Checked for Plagiarism: **Yes**

Language editor:

[Dr. Fatimah Ramezani](#)

Editor who approved publication:

[Dr. Milad Ghani](#)

DOI: [10.48309/AJCA.2024.415865.1415](#)

### KEYWORDS

Adsorption  
Cadmium  
Olive stones  
Isotherms  
Kinetics

### ABSTRACT

Cadmium (Cd) is a hazardous heavy metal that presents substantial hazards to both human well-being and the ecosystem. To address this issue, biosorption, an environmentally friendly and cost-effective technique, utilizes biological materials to capture metal ions from contaminated water. In our research, we focused on developing a biosorbent material using olive stones powder (OSP), which is a readily available agricultural waste. Our study aimed to assess the OSP effectiveness in the process of extracting Cd(II) ions from various aqueous solutions under diverse experimental parameters. In addition, we examined the adsorption kinetics and isotherms using various models. The findings revealed that OSP exhibited a strong adsorption capacity and affinity for Cd(II) ions, with a maximum value of 20.245 mg/g achieved at pH 6, an OSP dosage of 0.05 g, and a contact time of 30 minutes. The adsorption process adhered to the pseudo-second-order kinetic model and conformed to the Freundlich isotherm model, indicating the formation of multiple layers and the presence of heterogeneous surface sites. Furthermore, comparing the maximum capacity value ( $Q_m$ ) of OSP obtained in our study with previous research, it falls within the intermediate range. Overall, our study demonstrated the potential of OSP as a highly effective biosorbent material for effectively eliminating Cd(II) ions from aqueous solutions.

\* Corresponding author: Elsherif, Khaled Muftah

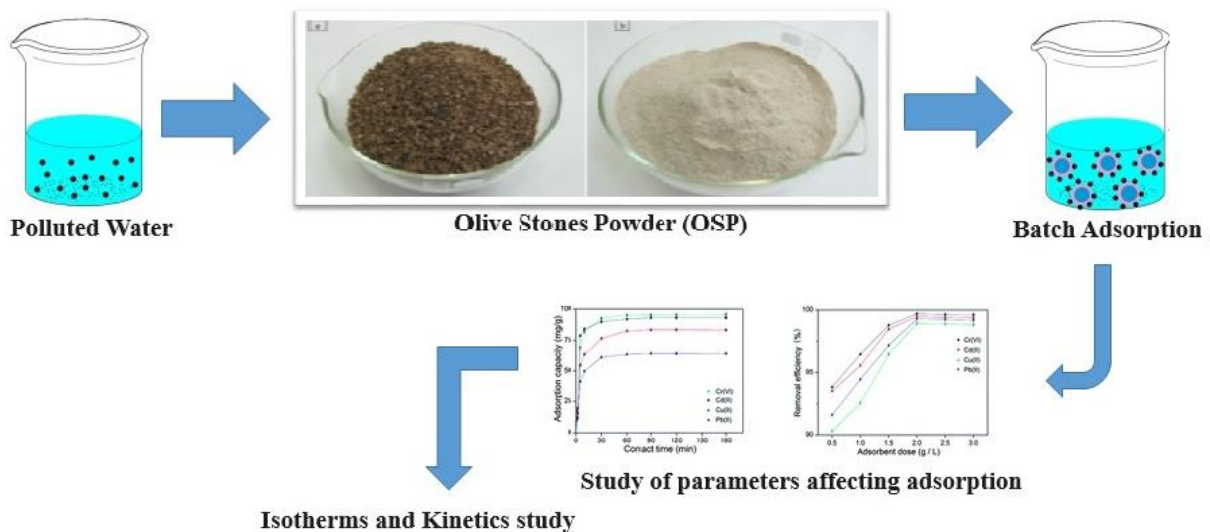
✉ E-mail: [elsherif27@yahoo.com](mailto:elsherif27@yahoo.com)

© 2024 by SPC (Sami Publishing Company)

---

**GRAPHICAL ABSTRACT**


---


**Introduction**

Water pollution is a critical issue that has far-reaching effects on all living organisms, primarily caused by the discharge of wastewater from diverse sources such as industries, landfills, and smaller enterprises [1,2]. One of the major contributors to this pollution is the occurrence of harmful metal ions in the wastewater [3]. These metals, which include cadmium, mercury, lead, copper, zinc, and chromium, are both non-biodegradable and toxic, posing a significant risk as they can enter the food chain and accumulate in organisms' bodies [4,5].

Cadmium (Cd) is a very toxic heavy metal that endangers humans, animals, and plants [6]. It has the capacity to quickly accumulate in the food chain, causing negative effects on different bodily systems in humans, including the neurological, pulmonary, renal, hepatic, and reproductive systems. Furthermore, it can impair growth, bone metabolism, and potentially contribute to cancer formation [7-9]. The World Health Organization (WHO) has classified cadmium as a priority pollutant due to its harmful effects, and the United States Environmental Protection Agency (EPA) has established a regulatory limit for

cadmium in both drinking water and industrial wastewater, with a maximum allowable concentration of 0.003 mg/L [10,11]. Cadmium can be found in the environment through a variety of sources, including recycling, coatings (e.g., galvanoplasty), battery manufacture, alloy manufacturing, solar cell production, pigments, and plastic stabilizers. As a result of its ubiquitous presence and accompanying hazards, the removal of cadmium has become a hot subject [12-14].

Several traditional methods exist for removing cadmium from contaminated aqueous solutions, including chemical oxidation or reduction, filtration, chemical precipitation, ion exchange, evaporative recovery, and electrochemical treatment [15-18]. However, these methods may not be highly effective when dealing with solutions containing cadmium concentrations below 100 mg/L. In such cases, the use of specific biomass offers an efficient, cost-effective, and user-friendly alternative [19-21].

The capacity of biomass, which consists of non-living and inert biological matter, to adsorb hazardous metals from aqueous environments via physicochemical processes that involves the

interaction between metal ions and binding sites present on biomass is commonly known as biosorption. Ion exchange, complex formation, precipitation, electrostatic interactions, and other processes are included [22,23]. There is information in the literature on several biosorbents obtained from agricultural waste that have been used to remove Cd(II) and other heavy metals. Palm leaves, tea and coffee waste powder, Phyllanthus emblica fruit stone, avocado pear exocarp, rice husk, Acacia plant, olive leaves, olive branches, orange peels, mesembryanthemum, and moringa oleifera leaves are some instances [24-33].

Olive stone, a type of lignocellulosic material, contains components such as hemicellulose, cellulose, lignin, and substantial quantities of phenolic compounds and protein. It is a significant byproduct generated during olive oil production, resulting in the generation of thousands of tons of waste annually [34]. Typically, olive stone exhibits a small particle size due to the crushing process involved in olive oil production. While this waste is often considered an environmental concern when improperly disposed of, utilizing plant waste for industrial purposes can contribute to reducing greenhouse gas emissions [35]. Moreover, agricultural waste products require lower water consumption compared to forest products. As a result, the value of olive stone as a valuable resource has gained significant attention, with studies demonstrating its potential as an adsorbent for metal ions in water solutions [36].

The objective of this work was to create a biosorbent material out of olive stones and test its efficiency in removing Cd(II) ions from aqueous solutions. The investigation also aimed to assess the impact of various experimental parameters, including the initial concentration of Cd(II), the duration of sorption, pH of solution, and adsorbent dose. The study also explored adsorption kinetics and isotherms to acquire a better understanding of the process.

## Experimental

### *Chemicals and Instruments*

In this study, high-quality chemicals and reagents were employed, including cadmium chloride, hydrochloric acid, and sodium hydroxide, all of which were of analytical grade. Standard laboratory procedures were followed to prepare the standard solution for each metal. All necessary solutions were prepared using analytical reagents, and deionized water was used exclusively throughout the experiment. Throughout the study, a pH meter (Hanna pH-209) from Hanna Company, a shaker (Shaker KS 15) from Edmund Bühler GmbH, and a drying oven (DOD-50) from RAYPA were utilized.

### *Biosorbent preparation*

The olive stones utilized in this study were obtained from local olive mills in Libya's Msallata region. To begin preparing the olive stones powder (OSP), they were rinsed with tap water to remove surface dust and contaminants. To guarantee complete cleaning, distilled water was used to rinse. Following that, the olive stones were air-dried before being baked in an oven at 70 °C until a consistent mass was attained. After drying, the biomass was pulverized and put through an electromagnetic filter to get particle sizes less than 500 µm. To maintain its integrity and protect it from moisture, the dried biomass was carefully stored in air-tight polyethylene container, ensuring its readiness for analysis. It is important to note that the adsorbent was utilized in its natural form without any modifications [33].

### *Batch Adsorption Experiments*

The influence of crucial experimental variables on the adsorption process was examined through batch experiments, following the methodology described by Alkherraz *et al.* [3]. This study

explored the effects of pH, contact time, dose, and initial metal ion concentrations. The solution's temperature, volume, and agitation rate were held constant at  $25 \pm 1$  °C, 50 mL, and 175 rpm, respectively.

#### *pH Effect*

The pH of the stock solution was changed using either 0.1 M HCl or NaOH to establish the ideal pH for maximal cadmium(II) adsorption using OSP. In each experiment, 50 mL of 50 mg/L cadmium(II) solution was mixed with 0.1 g of OSP in 150 mL Erlenmeyer flasks. The solution's original pH ranged from 2 to 8. The mixtures were then agitated at 175 rpm for 30 minutes while maintaining a temperature of  $25 \pm 1$  °C. The ultimate pH of each combination was recorded once equilibrium was reached. The samples were then filtered, and the concentrations of the filtrates were determined [21].

#### *Biosorbent dosage effect*

Separate 150 mL Erlenmeyer flasks were prepared, each containing 50 mL of Cd(II) ion solutions with a concentration of 50 mg/L. Different amounts of biosorbent, ranging from 0.05 to 1.00 g, were added to each flask. The mixtures were subsequently stirred on a shaker at 150 rpm for 30 minutes, maintaining a temperature of  $25 \pm 1$  °C and a pH of 6.0. Afterward, the mixtures were filtered, and the residual metal ions were analyzed [21].

#### *Contact time effect*

The adsorption experiments were conducted in a set of Erlenmeyer flasks, each containing 0.1 g of biosorbent and 50 mL of a Cd(II) ion solution with a concentration of 50 mg/L. The solutions were agitated in a water bath at a controlled temperature of  $25 \pm 1$  °C and an agitation rate of 175 rpm, while maintaining a pH of 6. Samples were collected at regular intervals (0-60

minutes) to monitor the progress of the adsorption process [21].

#### *Initial metal ion concentration effect*

Under optimized conditions, the impact of initial metal ion concentrations on adsorption was investigated. To achieve this, 0.1 g of OSP was combined with 50 mL of Cd(II) solutions ranging in starting concentrations from 10 to 100 mg/L, while maintaining a pH of 6.0. The experiments were conducted for 30 minutes at a constant temperature of  $25 \pm 1$  °C and a shaking rate of 175 rpm. Subsequently, the samples were filtered, and the residual metal ions were quantified using an atomic absorption spectrophotometer [21].

#### *Removal efficiency and adsorption capacity*

For every trial, the initial concentration of Cd(II) was measured using a Flame Atomic Absorption Spectrophotometer (Analytik Jena-novAA 800 F) both before and after the adsorption process. The adsorption capacity ( $Q_e$ ) and removal efficiency (%R) were calculated using Equations (1) and (2), respectively [9]:

$$Q_e = \frac{(C_o - C_e) \times V}{M} \quad (1)$$

$$\%R = \frac{C_o - C_e}{C_o} \times 100 \quad (2)$$

Where,  $C_o$  and  $C_e$  (in mg/L) indicate the starting and equilibrium final concentrations of Cd(II) in the equations, respectively. The solution volume is represented by V (in L), and the biosorbent mass is denoted as M (in g). The experiments were conducted in triplicate, and the mean values along with their corresponding standard deviations are reported.

#### *Data Analysis*

The equilibrium and kinetic data obtained from the sorption of Cd(II) ions onto the OSP adsorbent were subjected to analysis using the equilibrium and kinetic models specified in this

study. Various fitting parameters were utilized to establish correlations with the experimental data. The selection of the most appropriate model was based on the correlation coefficient, where the model with an  $R^2$  value closest to unity was deemed the best fit.

## Results and discussion

### *Impact of pH on Cd(II) adsorption*

The aqueous solution pH plays a crucial role in influencing the adsorption process [37]. To examine the impact of pH on the adsorption of cadmium (II) onto the OSP, the pH was systematically varied within the range of 2 to 8. The results depicted in Figure 1 demonstrate a clear trend, indicating that cadmium adsorption increased with the rise in pH from 2 to 6. However, beyond pH 6, the adsorption capacity declined. Notably, the highest adsorption of Cd(II) was observed at pH 6. The OSP exhibited a removal efficiency of 72.3% for Cd(II) at a pH of 6.05.

The adsorbent's ability to remove metal ions is influenced by the pH of the solution, which is determined by both the ion's nature and the properties of the material. The pH of a solution has an impact on the concentration and solubility of metal ions, as well as the presence of

counterions on the functional groups of the adsorbent. Under acidic conditions or at low pH levels (below 2), the concentration of  $H^+$  ions in the solution increases, leading to a higher degree of protonation of the active sites or functional groups on the surface of the OSP adsorbent. This protonation prevents metal ions from forming connections with active sites [4,7].

Within the mild pH range of 2 to 6, the active sites on the OSP adsorbent produced coupled  $H^+$  ions, increasing metal ion adsorption [38]. Precipitation became the dominating mechanism at pH values greater than 6.5. Furthermore, ion exchange and the creation of aqueous metal hydroxides may occur at faster rates. However, because to electrostatic repulsion, these complexes were rejected by the negatively charged OSP particles. This process explains why metal ion elimination is reduced at pH values over 6.5 [39]. The results obtained agreed with the results given by Berhe [40]. Another investigation on the adsorption properties of metal ions done by Habib et al. [41] found that the highest adsorption effectiveness was seen within the pH range of 2-10. This phenomenon can be attributed to the interaction between the metal ions and the functional groups or active sites present on the surface of the adsorbent [4].

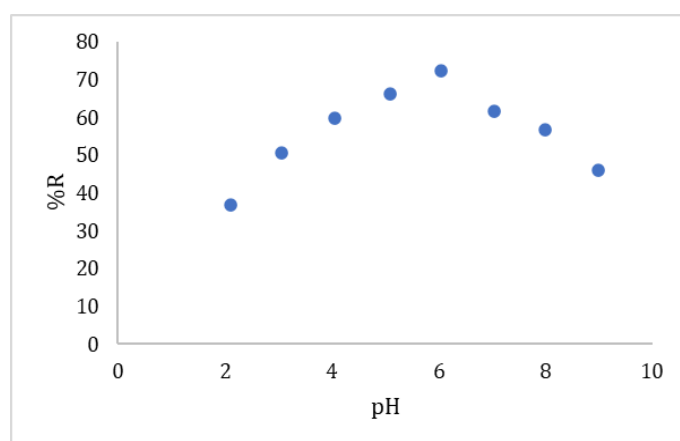


**Figure 1.** Effect of pH on the adsorption of Cd(II) onto OSP.

### *Impact of biosorbent dosage on Cd(II) adsorption*

The impact of OSP dose on the adsorption capacity ( $Q_e$ ) and removal efficiency (%R) of Cd(II) is illustrated in Figure 2. As the OSP dose increases from 0.05 to 1.0 g, the %R rises. Within this dose range, however, the  $Q_e$  drops. The %R is 75% at 0.05 g, and it reaches the maximum removal value of 89% at 1.0 g. This is a consequence of the augmented surface area, leading to an increase in the availability of biosorption sites [21]. All adsorbent sites are fully occupied at smaller doses (0.05 g), resulting in surface saturation and a high  $Q_e$  value (~38 mg/g). However, at 1.0 g doses, the splitting effect of the concentration gradient between the biosorbent and the sorbate causes a considerable drop in  $Q_e$ . The decrease in  $Q_e$  corresponds to a reduction in the amount of Cd(II) adsorbed per unit mass of OSP. In addition, an increase in biosorbent dose can potentially result in agglomeration and blockage of accessible adsorption sites, thereby restricting the contact between the metal and the OSP surface [42]. Based on these findings, a dose of 0.05 g of OSP was determined to be the best value for providing an appropriate surface area for Cd(II) adsorption.

### *Impact of contact time on Cd(II) adsorption*

The influence of contact time on the adsorption of Cd(II) ions onto OSP is illustrated in Figure 3. Initially, when contact duration rose from 0 to 20 minutes, removal efficiency improved. The adsorption process, on the other hand, grew reasonably steady over time. Equilibrium clearance of Cd(II) ions was achieved in approximately 30 minutes, and further increases in contact time did not lead to significant additional adsorption. The contact duration of 30 minutes was utilized in all experiments to ensure the maximum removal efficiency. The initial rapid rate of removal can be attributed to the

smaller ionic radius of Cd(II) ions, facilitating faster diffusion to the OSP surface [21]. The rapid adsorption observed in the early stages is likely due to the abundance of active sites on the OSP surface, which gradually become saturated over time. With the decrease in available active sites, the early stages of sorption are likely governed by diffusion from the bulk solution to the adsorbent's surface, while the later stages are predominantly controlled by attachment mechanisms [30].

### *Impact of initial concentration on Cd(II) adsorption*

The initial concentration of the metal ion plays a crucial role in determining the extent of metal ion adsorption, making it a crucial factor for achieving successful adsorption [22]. In this study, the adsorption capacity of OSP for Cd(II) ions increased as the metal ion concentrations ranged from 10 to 100 mg/L. This increase in concentration created a steeper metal ion concentration gradient, which facilitated overcoming resistance to mass transfer between the aqueous phase and the adsorbent [43]. A higher concentration in the solution indicates a larger number of metal ions available for binding to the adsorbent's surface. The significant adsorption capacity of OSP for Cd(II) ions can be attributed to its surface porosity, as demonstrated in Figure 4. In addition, its high surface area and strong cation exchange ability contribute to its enhanced adsorption capacity [21]. Similar findings were reported by Dowodu and Okpomie [44], who investigated the sequential adsorption of Ni(II) and Mn(II) ions from an aqueous solution using Nigerian kaolinite clay. Higher metal concentrations led to faster saturation of the adsorbent sites, resulting in a lower overall percentage of metal removal. This trend aligns with the observations of [43].

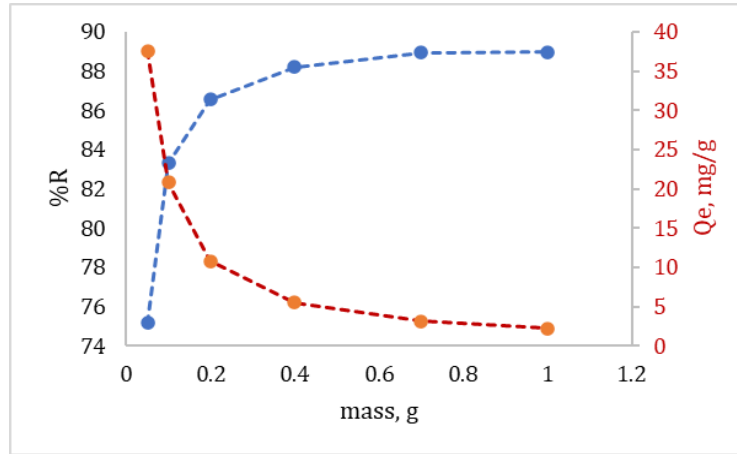


**Figure 2.** OSP dosage effect on the adsorption capacity ( $Q_e$ ) and removal efficiency (%R) of Cd(II).

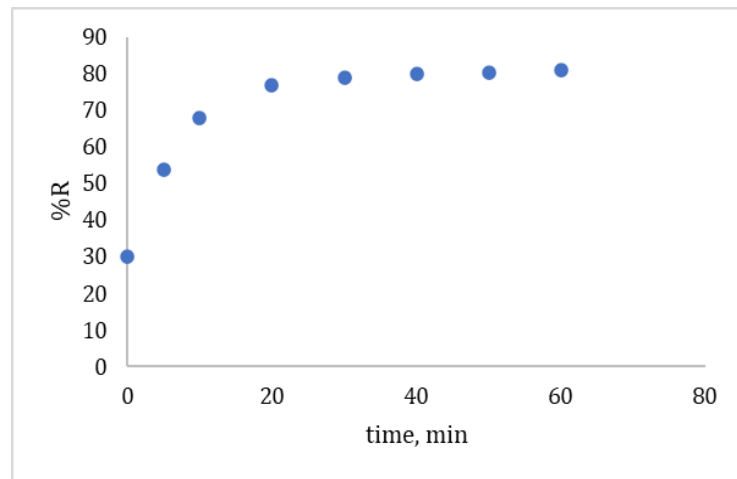


**Figure 3.** Effect of contact time on the adsorption of Cd(II) onto OSP.

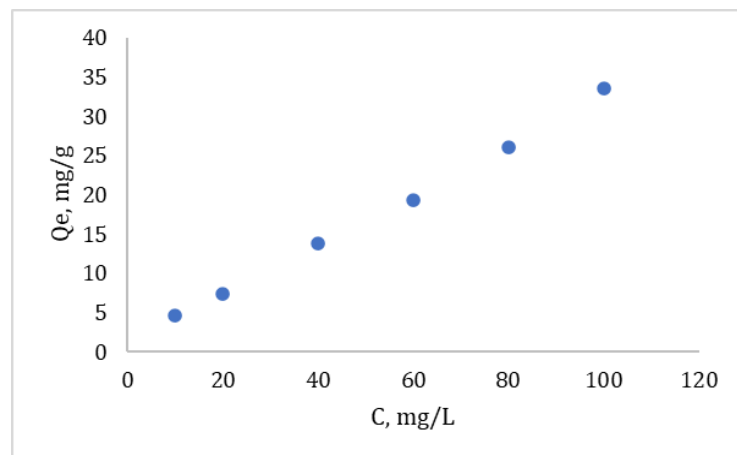


**Figure 4.** Effect of initial concentration on the adsorption of Cd(II) onto OSP.

### Kinetic Study

To investigate the kinetics of the adsorption process, the experimental adsorption data of Cd(II) onto OSP were examined using three models: the Pseudo-First-Order, Pseudo-Second-Order, and Elovich models [22,45-47]. The results of linear form calculations, utilizing Equations (3) to (6), are presented in Figures 5, 6, and 7.

The Lagergren's Pseudo-First-Order kinetic rate expression is given by the following form [22]:

$$\frac{1}{Q_t} = \frac{k_1}{Q_e \times t} + \frac{1}{Q_e} \quad (3)$$

Lagergren's pseudo-first-order kinetic rate expression is given by the equation, where  $Q_t$  and  $Q_e$  (mg/g) represent the adsorbed quantities of Cd(II) at time  $t$  and equilibrium, respectively. The parameter  $k_1$  ( $\text{min}^{-1}$ ) denotes the adsorption rate constant. To evaluate the pseudo-first-order model, the plot of  $\ln(Q_e - Q_t)$  against time ( $t$ ) was extrapolated using Equation (4) [45].

$$\ln(Q_e - Q_t) = \ln(Q_e) - \frac{k_1}{2.303} \times t \quad (4)$$

The investigation of pseudo-second-order kinetics involved extrapolating the plot of  $(t/Q_t)$  against time ( $t$ ), as described by Equation (5) [46].

$$\frac{t}{Q_t} = \frac{1}{k_2 \times Q_e^2} + \frac{t}{Q_e} \quad (5)$$

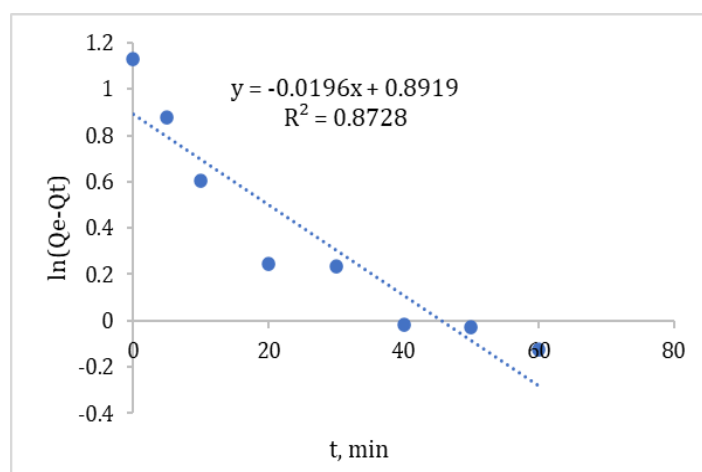
In Equation (5), the parameter  $k_1$  ( $\text{g.mg}^{-1}.\text{min}^{-1}$ ) represents the adsorption rate constant.

The linear form of the Elovich model can be expressed using Equation (6) [47]:

$$Q_t = \frac{1}{\beta} \ln(\alpha\beta) + \frac{1}{\beta} \ln(t) \quad (6)$$

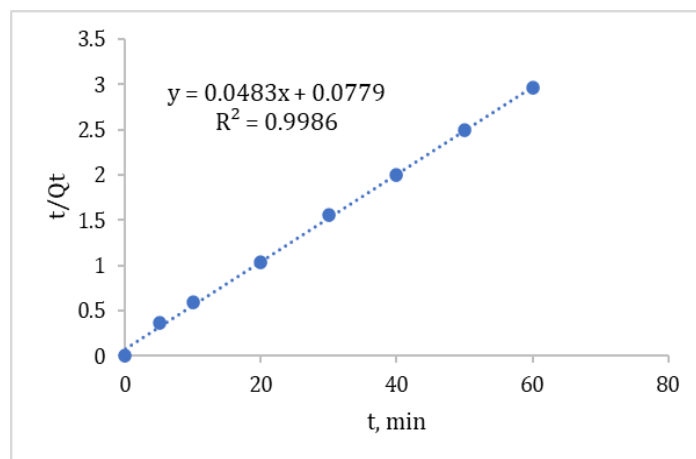
In the context of the Elovich model, the parameter  $\alpha$  ( $\text{mg.g}^{-1}.\text{min}^{-1}$ ) represents the initial adsorption rate, while the parameter  $b$  ( $\text{g.mg}^{-1}$ ) is associated with the desorption constant specific to each experiment.

Table 1 presents the adsorption characteristics obtained from Figures 5, 6, and 7, which provide insights into the agreement between the results and the investigated mechanism. The correlation coefficient ( $R^2$ ), which approaches 1 when the model fits the data, indicates the goodness of fit of the model. Among the kinetic models examined, the pseudo-second-order model exhibited the best fit. The calculated values of  $Q_e$  using this model (20.704 mg/g) were highly comparable to the experimentally derived  $Q_e$  values (20.245 mg/g) for OSP. This suggests that the pseudo-second-order model provides a more accurate representation of the adsorption of Cd(II) ions onto olive stone powder.



**Figure 5.** Pseudo-First-Order graph for the adsorption of Cd(II) onto OSP.





**Figure 6.** Pseudo-Second-Order graph for the adsorption of Cd(II) onto OSP.

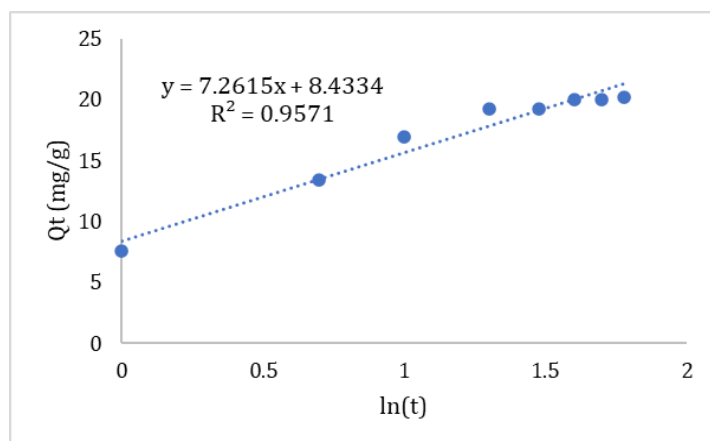


**Figure 7.** Elovich model graph for the adsorption of Cd(II) onto OSP.

**Table 1.** Kinetic parameters for Cd(II) adsorption onto OSP

<b>Pseudo-First-Order</b>			
$k_1$ ( $\text{min}^{-1}$ )	$Q_e$ (Cal.) ( $\text{mg}\cdot\text{g}^{-1}$ )	$R^2$	$Q_e$ (Exp.) ( $\text{mg}\cdot\text{g}^{-1}$ )
<b>0.045</b>	7.797	0.8728	20.245
<b>Pseudo-Second-Order</b>			
$k_2$ ( $\text{g}\cdot\text{mg}^{-1}\cdot\text{min}^{-1}$ )	$Q_e$ (Cal.) ( $\text{mg}\cdot\text{g}^{-1}$ )	$R^2$	$Q_e$ (Exp.) ( $\text{mg}\cdot\text{g}^{-1}$ )
<b>0.030</b>	20.704	0.9986	20.245
<b>Elovich</b>			
$\beta$ ( $\text{g}\cdot\text{mg}^{-1}$ )	$\alpha$ ( $\text{mg}\cdot\text{g}^{-1}\cdot\text{min}^{-1}$ )	$R^2$	$Q_e$ (Exp.) ( $\text{mg}\cdot\text{g}^{-1}$ )
<b>0.138</b>	105.711	0.9571	20.245

#### *Isotherm Study*

Figure 8 illustrates the adsorption isotherms of Cd(II) ions onto the OSP adsorbent at room temperature. These isotherms provide insights

into the interaction between metal ions and adsorbents, which are crucial factors in determining the effectiveness of adsorption processes [22]. The residual concentration of the adsorbate in the solution ( $C_e$ , mg/L) was utilized

to calculate the amount of adsorbate on the adsorbent ( $Q_e$ , mg/g). The quantity of adsorbed Cd(II) ions increased proportionally with the initial concentration ( $C_o$ ). The data indicated that the adsorption process was initially rapid, followed by a gradual slowdown until it reached a plateau, indicating saturation of the porous surfaces. The closer alignment of Cd(II) ion adsorption onto OSP with the predicted line, indicating 100% adsorption within the lower  $C_o$  range, demonstrated a stronger affinity between Cd(II) ions and the OSP adsorbent.

Various isotherm equations have been employed to describe the equilibrium behavior of adsorption. In this study, the adsorption data were analyzed, and the Langmuir, Freundlich, Temkin, and Dubinin-Kaganer Radushkevich (D-R) equations [48-51] were fitted to the data. The estimated parameters of the isotherm models are presented in Figures 9, 10, 11, and 12. The Langmuir adsorption isotherm, which assumes monolayer adsorption occurring exclusively on the homogeneous surface of the adsorbent, was linearly transformed and is represented by Equation (7) [25].

$$\frac{1}{Q_e} = \frac{1}{Q_m} + \frac{1}{b Q_m C_e} \quad (7)$$

Where,  $Q_e$  (mg/g) and  $C_e$  (mg/L) denote the adsorbate's adsorption capacity and equilibrium concentration, respectively. The maximal

adsorption capacity of OSP is denoted by  $Q_m$  (mg/g), whereas the Langmuir constant is represented by  $b$  (L/mg).

The linear transformation of the Freundlich adsorption isotherm is presented in Equation (8), which explains the multilayer adsorption process and accounts for interactions between adsorbed molecules and heterogeneous surfaces [29]:

$$\log Q_e = \log K_F + \frac{1}{n} \log C_e \quad (8)$$

The Freundlich adsorption constants,  $n$  and  $K_F$  (mg/g (L/mg)<sup>1/n</sup>), are connected with the adsorption intensity and capacity, respectively, in the equation. The value of  $n$  represents the adsorption process's divergence from linearity. If  $n < 1$ , it represents a chemical adsorption process. If  $n = 1$ , the adsorption process is linear. If  $n > 1$ , it indicates a physical adsorption process.

Equation (9) represents the linear modification of the Temkin adsorption isotherm. This isotherm considers both the influence of indirect interactions between the adsorbate and adsorbent on the adsorption process and assumes a linear decline in the heat of adsorption for all molecules as the adsorbed molecular layer becomes saturated [33].

$$Q_e = B_T \ln K_T + B_T \ln C_e \quad (9)$$

The equation includes the Temkin adsorption constant ( $B_T$ , J.mol<sup>-1</sup>) and the Temkin isotherm constant ( $K_T$ , L.mg<sup>-1</sup>).

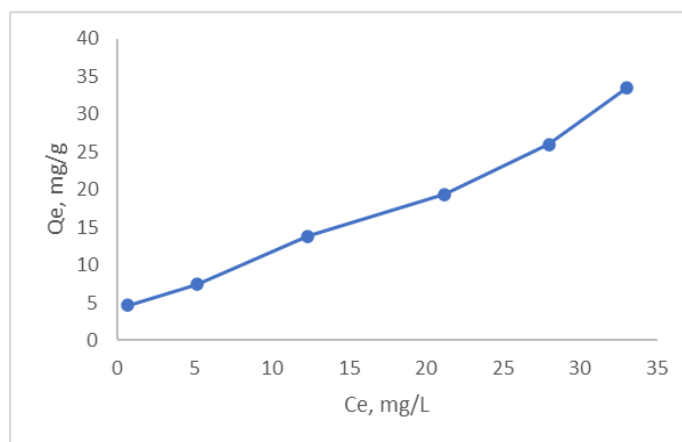


**Figure 8.** Adsorption isotherm of Cd(II) ions onto OSP.

The Dubinin-Kaganer Radushkevich (Dubinin-Radushkevich) adsorption isotherm approach is frequently used to explain the adsorption mechanism on non-uniform surfaces with a Gaussian energy distribution. The Dubinin-Radushkevich adsorption isotherm, unlike other isotherm models, does not presuppose a

homogenous surface or constant adsorption potentials. It can, however, estimate the apparent energy of absorption. The following equation [17] is the linearized form of the Dubinin-Radushkevich isotherm:

$$\log Q_e = \log Q_m - \beta \varepsilon^2 \quad (10)$$

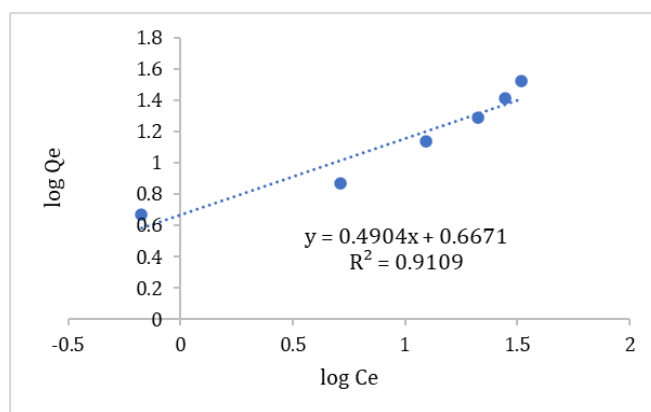


**Figure 9.** Freundlich isotherm plot for adsorption of Cd(II) onto OSP

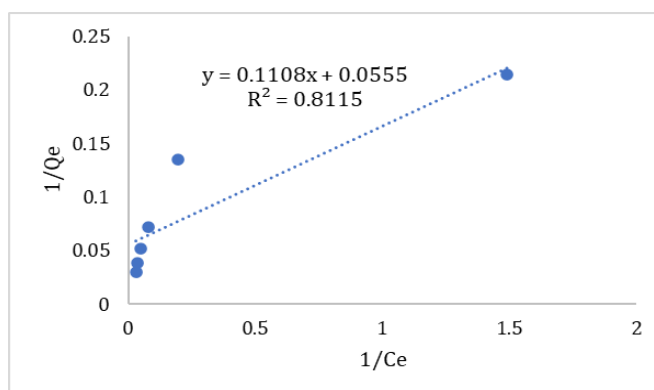


**Figure 10.** Langmuir isotherm plot for adsorption of Cd(II) onto OSP.

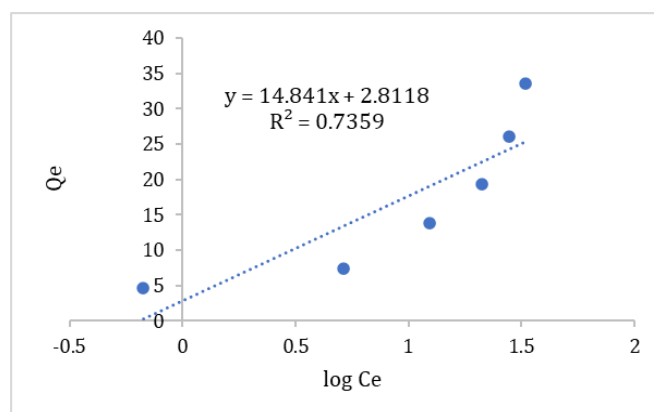


**Figure 11.** Temkin isotherm plot for adsorption of Cd(II) onto OSP.

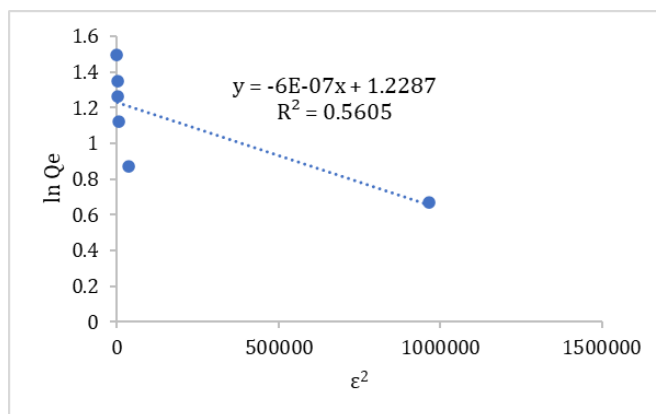


**Figure 12.** Dubinin-Radushkevich isotherm plot for adsorption of Cd(II) onto OSP.

Where,  $\beta$  ( $\text{mol}^2/\text{J}^2$ ) is the Dubinin-Radushkevich constant, which relates to the characteristic energy of adsorption and  $\varepsilon$  ( $\text{J}/\text{mol}$ ) is the Polanyi potential, which is a measure of the potential energy of adsorption per mole of adsorbate.

The obtained parameters and correlation coefficients resulting from the application of the Langmuir, Freundlich, Temkin, and Dubinin-Radushkevich models to the adsorption of Cd(II) ions onto Olive Stones Powder (OSP) are summarized in Table 2. The correlation coefficient, denoted as  $R^2$ , indicates the goodness of fit of the model to the experimental data. In this case, the Freundlich model exhibited the highest correlation coefficient, reaching 0.90.

This suggests that the Freundlich model, which considers multilayer adsorption and the attachment of adsorbed molecules through hydrophobic or weak interactions, reliably represents the adsorption isotherm for Cd(II) from OSP. The substantial correlation coefficients further support the applicability of the Freundlich model in describing the adsorption behavior of Cd(II) ions on OSP.

The Freundlich model parameters,  $K_F = 4.646 \text{ mg/g (L/mg)}^{1/n}$  and  $n = 2.039$  ( $n > 1$ ), imply that Cd(II) biosorption onto OSP is favorable. These results indicate that the adsorption process has numerous layers and is characterized by a high affinity between the adsorbate and adsorbent.

**Table 2.** Langmuir, Freundlich, Temkin, and Dubinin-Radushkevich isotherm model parameters for Cd(II) adsorption onto OSP

Model	Parameter	Value
Langmuir	b (L/mg)	0.501
	$Q_m$ (mg/g)	18.108
	$R^2$	0.8115
Freundlich	$K_F$ ( $\text{mg/g (L/mg)}^{1/n}$ )	4.646
	n	2.039
	$R^2$	0.9109
Temkin	$B_T$ (J/mol)	14.841
	$K_T$ (L/mg)	1.547
	$R^2$	0.7659
Dubinin-Radushkevich	$Q_m$ (mg/g)	16.932
	$\beta$ ( $\text{mol}^2/\text{J}^2$ )	$6 \times 10^{-7}$
	$R^2$	0.5605

**Table 3.** Comparison of Cd(II) Biosorption Capacity ( $Q_m$ ) in Present Study with Previous Published Works

Biosorbent Dosage (g/L)	$Q_m$ (mg/g)	Reference
2.00	20.25	Present Study
1.00	58.50	9
3.00	25.86	52
3.00	24.00	53
5.00	20.60	54
0.50	13.91	27
5.00	155.90	55
10.00	12.15	56
6.70	30.21	57
6.70	34.84	57
20.00	4.42	58
1.00	3.15	24
3.00	29.00	59
2.50	7.24	60
2.50	11.00	61

The Langmuir model, on the other hand, demonstrates that Cd(II) biosorption onto OSP follows a monolayer formation mechanism. The maximal adsorption capacity of the model is  $Q_m = 18.108$  mg/g, and the affinity constant is  $b = 0.501$  L/mg. The low affinity constant value shows typical sorbate-sorbent interactions seen in physisorption processes.

Table 3 presents the maximum Cd(II) biosorption capacities,  $Q_m$ , of various biomasses similar to the one examined in this study. The  $Q_m$  value for OSP falls within the intermediate range, suggesting that this material is well-suited for the effective removal of Cd(II) from aqueous solutions.

## Conclusion

The findings of this study demonstrate the potential of OSP as an effective biosorbent material for the removal of Cd(II) ions from aqueous solutions. The study examined the influence of various experimental factors, including initial Cd(II) concentration, sorption time, solution pH, and adsorbent dosage, on the adsorption process. It was determined that pH 6,

an OSP dosage of 0.05 g, and a contact time of 30 minutes were the optimal conditions for Cd(II) removal.

The kinetics and isotherms of the adsorption process were also investigated using several models in the study. The pseudo-second-order model and the Freundlich model exhibited the best fit to the experimental data, as indicated by the correlation coefficients ( $R^2$ ). These results suggest that the adsorption process involves the formation of multiple layers and occurs at heterogeneous surface sites.

Furthermore, the study revealed that OSP possesses a high adsorption capacity and strong affinity for Cd(II) ions, making it a promising biosorbent material for environmental applications.

## Acknowledgment

We would like to extend our gratitude to the Chemistry Department, Faculty of Arts and Science, Elmergib University for their support and resources in conducting this research. Their contribution has been instrumental in the successful completion of this work.


## Disclosure statement

The authors declare that there are no relevant competing interests to disclose with respect to this research study.

## Orcid

Khaled M. Elsherif : 0000-0002-3884-1804

Rima A. A. Saad : 0009-0000-5482-2112

Abdunaser M. Ewlad-Ahmed : 0000-0002-1897-8328

Abdullah A. Treban : 0009-0004-3412-8974

Abdulrhman M. Iqneebir : 0009-0004-7868-4024

## References

- [1] R.B. Gameli, E.H. Alhassan, A.B. Duwiejuah, E.D. Abarike, A.A. Bawa, *S. Afr. J. Sci.*, **2023**, *119*, 1–9. [[CrossRef](#)], [[Google Scholar](#)], [[Publisher](#)]
- [2] H.N. Tran, S.J. You, A. Hosseini-Bandegharai, H.P. Chao, *Water Res.*, **2017**, *120*, 88–116. [[CrossRef](#)], [[Google Scholar](#)], [[Publisher](#)]
- [3] A.M. Alkherraz, A.K. Ali, K.M. Elsherif, *Chem. Int.*, **2020**, *6*, 11–20. [[CrossRef](#)], [[Google Scholar](#)], [[Publisher](#)]
- [4] M.T. Yifira, M.B. Doda, C.K. Kanido, *Pak. J. Anal. Environ. Chem.*, **2023**, *24*, 106–117. [[CrossRef](#)], [[Google Scholar](#)], [[Publisher](#)]
- [5] K.M. Elsherif, A. El-Hashani, A. El-Dali, M. Saad, *Int. J. Chem. Pharm. Sci.*, **2014**, *2*, 890–897. [[Google Scholar](#)]
- [6] M. Elsherif, Z.Y. Alzalouk, A. Zubi, S.A.S. Al-Ddarwish, *Chem. Int.*, **2022**, *8*, 144–152. [[CrossRef](#)], [[Google Scholar](#)]
- [7] M. Naushad, M.R. Khan, T. Ahamad, *Desalin. Water Treat.*, **2023**, *293*, 208–215. [[CrossRef](#)], [[Google Scholar](#)]
- [8] G.T. Tee, X.Y. Gok, W.F. Yong, *Environ. Res.*, **2022**, *212*, 113248. [[CrossRef](#)], [[Google Scholar](#)], [[Publisher](#)]
- [9] C. Lavado-Meza, L. De la Cruz-Cerrón, C. Lavado-Puente, F. Gamarra-Gómez, E. Sacari-Sacari, J.Z. Dávalos-Prado, *Molecules*, **2023**, *28*, 5491. [[CrossRef](#)], [[Google Scholar](#)], [[Publisher](#)]
- [10] Y. Zheng, S. Yu, Y. Li, J. Peng, J. Yu, R. Chi, C. Xiao, *Biochem. Eng. J.*, **2022**, *187*, 108667. [[CrossRef](#)], [[Google Scholar](#)], [[Publisher](#)]
- [11] H.A. Saeed, N.Y. Harun, M.M. Nasef, A. Al-Fakih, A.A.S. Ghaleb, H.K. Afolabi, *Ain Shams Eng. J.*, **2022**, *13*, 101516. [[CrossRef](#)], [[Google Scholar](#)], [[Publisher](#)]
- [12] H. Nabipour, S. Rohani, S. Batool, A.S. Yusuff, *J. Environ. Chem. Eng.*, **2023**, *11*, 109131. [[CrossRef](#)], [[Google Scholar](#)], [[Publisher](#)]
- [13] A.R. Weshahy, A.K. Sakr, A.A. Gouda, B.M. Atia, H.H. Somaily, M.Y. Hanfi, M.I. Sayyed, R. El Sheikh, E.M. El-Sheikh, H.A. Radwan, M.F. Cheira, M.A. Gado, *Int. J. Mol. Sci.*, **2022**, *23*, 8677. [[CrossRef](#)], [[Google Scholar](#)], [[Publisher](#)]
- [14] A.M. Alkherraz, A.K. Ali, K.M. Elsherif, *J. Med. Chem. Sci.*, **2020**, *3*, 1–10. [[CrossRef](#)], [[Google Scholar](#)], [[Publisher](#)]
- [15] H. Qin, T. Hu, Y. Zhai, N. Lu, J. Aliyeva, *Environ. Pollut.*, **2020**, *258*, 113777. [[CrossRef](#)], [[Google Scholar](#)], [[Publisher](#)]
- [16] K.M. Elsherif, M.M. Yaghi, *Moroc. J. Chem.*, **2017**, *5*, 131–138. [[CrossRef](#)], [[Google Scholar](#)], [[Publisher](#)]
- [17] A.M. Alkherraz, K.M. Elsherif, A. El-Dali, N.A. Blayblo, M. Sasi, *J. Med. Nanomater. Chem.*, **2022**, *5*, 118–131. [[CrossRef](#)], [[Publisher](#)]
- [18] A. Pathirana, N.S.L. Dissanayake, N.D. Wanasekara, B. Mahltig, G.K. Nandasiri, *Nanomaterials*, **2023**, *13*, 498. [[CrossRef](#)], [[Google Scholar](#)], [[Publisher](#)]
- [19] G.E. Hegazy, N.A. Soliman, M.E. Ossman, Y.R. Abdel-Fattah, M.N. Moawad, *Sci. Rep.*, **2023**, *13*, 2550. [[CrossRef](#)], [[Google Scholar](#)], [[Publisher](#)]
- [20] M. Asadullah, Q. Ain, F. Ahmad, *Adv. J. Chem. Sect. A.*, **2022**, *5*, 345–356. [[CrossRef](#)], [[Google Scholar](#)], [[Publisher](#)]
- [21] T.V. Silas, A.S. Osagie, *GSC Biol. Pharm. Sci.*, **2023**, *24*, 319–328. [[CrossRef](#)], [[Google Scholar](#)], [[Publisher](#)]

- [22] S. Zghal, I. Jedidi, M. Cretin, S. Cerneaux, M. Abdelmouleh, *Materials*, **2023**, *16*, 1015. [[CrossRef](#)], [[Google Scholar](#)], [[Publisher](#)]
- [23] W.T. Tee, N.Y.L. Loh, B.Y.Z. Hiew, S. Hanson, S. Thangalazhy-Gopakumar, S. Gan, L.Y. Lee, *Biochem. Eng. J.*, **2022**, *187*, 108629. [[CrossRef](#)], [[Google Scholar](#)], [[Publisher](#)]
- [24] S. Kushwaha, Suhas, M. Chaudhary, I. Tyagi, R. Bhutiani, J. Goscianska, J. Ahmed, Manila, S. Chaudhary, *Molecules*, **2022**, *27*, 3355. [[CrossRef](#)], [[Google Scholar](#)], [[Publisher](#)]
- [25] K.M. Elsherif, A.M.S. Ewlad-Ahmed, A.A.S. Treban, *Appl. J. Environ. Eng. Sci.*, **2017**, *3*, 341–352. [[CrossRef](#)], [[Google Scholar](#)], [[Publisher](#)]
- [26] K.M. Elsherif, A. El-Hashani, I. Haider, *Asian J. Green Chem.*, **2018**, *2*, 380–394. [[CrossRef](#)], [[Google Scholar](#)], [[Publisher](#)]
- [27] S. Rostamzadeh Mansour, N. Sohrabi-Gilani, P. Nejati, *Adv. J. Chem. Sect. A.*, **2022**, *5*, 31–44. [[CrossRef](#)], [[Google Scholar](#)], [[Publisher](#)]
- [28] M. Fawzy, M. Nasr, A.M. Abdel-Rahman, G. Hosny, B.R. Odhafa, *Int. J. Phytoremediat.*, **2019**, *21*, 1205–1214. [[CrossRef](#)], [[Google Scholar](#)], [[Publisher](#)]
- [29] K.M. Elsherif, A.M. Ewlad-Ahmed, A. Treban, *World J. Biochem. Mol. Biol.*, **2017**, *2*, 46–51. [[Google Scholar](#)], [[Publisher](#)]
- [30] M. Janighorban, N. Rasouli, N. Sohrabi, M. Ghaedi, *Adv. J. Chem. Sect. A., Special Issue*, **2020**, *3*, 701–721. [[CrossRef](#)], [[Google Scholar](#)], [[Publisher](#)]
- [31] M.T. Hossain, S. Khandaker, M.M. Bashar, A. Islam, M. Ahmed, R. Akter, A.K.D. Alsukaibi, M.M. Hasan, H.M. Alshammari, T. Kuba, M.R. Awual, *J. Mol. Liq.*, **2022**, *368*, 120810. [[CrossRef](#)], [[Google Scholar](#)], [[Publisher](#)]
- [32] A.M. Alkheraz, A.K. Ali, A. El-Dali, K.M. Elsherif, *Chem. J.*, **2019**, *6*, 8–17. [[Google Scholar](#)], [[Publisher](#)]
- [33] A.M. Alkheraz, K.M. Elsherif, N.A. Blyblo, *Chem. Int.* **2023**, *9*, 134–145. [[CrossRef](#)], [[Google Scholar](#)], [[Publisher](#)]
- [34] Y. Gao, M.C. Aliques Tomas, J. Garemark, X. Sheng, L. Berglund, Y. Li, *Front. Mater.*, **2021**, *8*, 605931. [[CrossRef](#)], [[Google Scholar](#)], [[Publisher](#)]
- [35] I. Vera, R. Hoefnagels, A. Kooij, C. Moretti, M. Junginger, *Biofuels Bioprod. Bioref.*, **2020**, *14*, 198–224. [[CrossRef](#)], [[Google Scholar](#)], [[Publisher](#)]
- [36] G. Rodríguez-Gutiérrez, F. Rubio-Senent, A. Lama-Muñoz, A. García, J. Fernández-Bolaños, *J. Agric. Food Chem.*, **2014**, *62*, 8973–8981. [[CrossRef](#)], [[Google Scholar](#)], [[Publisher](#)]
- [37] M.R.F. Oliveira, K. do Vale Abreu, A.L.E. Romão, D.M.B. Davi, C.E. de Carvalho Magalhães, E.N.V.M. Carrilho, C.R. Alves, *Environ. Sci. Pollut. Res.*, **2021**, *28*, 18941–18952. [[CrossRef](#)], [[Google Scholar](#)], [[Publisher](#)]
- [38] S.R. Taffarel, J. Rubio. *Miner. Eng.*, **2009**, *22*, 336–343. [[CrossRef](#)], [[Google Scholar](#)], [[Publisher](#)]
- [39] A.K. Giri, R. Patel, S. Mandal, *Chem. Eng. J.*, **2012**, *186*, 71–81. [[CrossRef](#)], [[Google Scholar](#)], [[Publisher](#)]
- [40] S. Berhe, D. Ayele, A. Tadesse, A. Mulu, *Int. J. Sci. Res. Publ.*, **2015**, *5*, P454621. [[CrossRef](#)], [[Google Scholar](#)]
- [41] A. Habib, N. Islam, A. Islam, A.M. Shafiqul Alam, *Pak. J. Anal. Environ. Chem.*, **2007**, *8*, 21–25. [[Google Scholar](#)], [[Publisher](#)]
- [42] N. Barka, M. Abdennouri, M.E. Makhfouk, S. Qourzal, *J. Environ. Chem. Eng.*, **2013**, *1*, 144–149. [[CrossRef](#)], [[Google Scholar](#)], [[Publisher](#)]
- [43] N. Kannan, T. Veemaraj, *Electron. J. Environ. Agric. Food Chem.*, **2010**, *9*, 327–336. [[Google Scholar](#)], [[Publisher](#)]
- [44] F.A. Dawodu, K.G. Akpomie, *J. Mater. Res. Technol.* **2014**, *3*, 129–141. [[CrossRef](#)], [[Google Scholar](#)], [[Publisher](#)]
- [45] K.M. Elsherif, A. El-Dali, A.M. Ewlad-Ahmed, A.A. Treban, H. Alqadhi, S. Alkarewi, *Moroccan J. Chem.*, **2022**, *10*, 639–651. [[CrossRef](#)], [[Google Scholar](#)], [[Publisher](#)]

- [46] X. Xing, H. Qu, R. Shao, Q. Wang, H. Xie, *Water Sci. Technol.*, **2017**, *76*, 1243–1250. [[CrossRef](#)], [[Google Scholar](#)], [[Publisher](#)]
- [47] R. Kamaraj, S. Vasudevan, *New J. Chem.*, **2016**, *40*, 2249–2258. [[CrossRef](#)], [[Google Scholar](#)], [[Publisher](#)]
- [48] R. Kamaraj, A. Pandiarajan, M.R. Gandhi, A. Shibayama, S. Vasudevan, *ChemistrySelect*, **2017**, *2*, 342–355. [[CrossRef](#)], [[Google Scholar](#)], [[Publisher](#)]
- [49] A.M.K. Aljebori, A.N. Alshirifi, *Asian J. Chem.*, **2012**, *24*, 5813. [[Google Scholar](#)], [[Publisher](#)]
- [50] D.L. Postai, C.A. Demarchi, F. Zanatta, D.C.C. Melo, C.A. Rodrigues, *Alex. Eng. J.*, **2016**, *55*, 1713–1723. [[CrossRef](#)], [[Google Scholar](#)], [[Publisher](#)]
- [51] R. Saadi, Z. Saadi, R. Fazaeli, N.E. Fard, *Korean J. Chem. Eng.*, **2015**, *32*, 787–799. [[CrossRef](#)], [[Google Scholar](#)], [[Publisher](#)]
- [52] H. Azarpira, Y. Mahdavi, D. Balarak, *Pharma Chem.*, **2016**, *8*, 61–67. [[Google Scholar](#)], [[Publisher](#)]
- [53] D. Balarak, H. Azarpira, F.K. Mostafapour, *Pharma Chem.*, **2016**, *8*, 243–247. [[Google Scholar](#)], [[Publisher](#)]
- [54] M.A. Hossain, H.H. Ngo, W.S. Guo, L.D. Nghiem, F.I. Hai, S. Vigneswaran, T.V. Nguyen, *Bioresour. Technol.*, **2014**, *160*, 79–88. [[CrossRef](#)], [[Google Scholar](#)], [[Publisher](#)]
- [55] A. Takdastan, S. Samarbaf, Y. Tahmasebi, N. Alavi, A.A. Babaei, *Int. J. Environ. Sci. Technol.*, **2019**, *78*, 352–363. [[CrossRef](#)], [[Google Scholar](#)], [[Publisher](#)]
- [56] B.I. Olu-Owolabi, O.U. Oputu, K.O. Adebowale, O. Ogunsolu, O.O. Olujimi, *Sci. Res. Essays.*, **2012**, *7*, 1614–1629. [[CrossRef](#)], [[Google Scholar](#)], [[Publisher](#)]
- [57] A.K.I. Flores-Trujillo, P. Mussali-Galante, M.C. de Hoces, G. Blázquez-García, H.A. Saldarriaga-Noreña, A. Rodríguez-Solís, E. Tovar-Sánchez, E. Sánchez-Salinas, L. Ortiz-Hernández, *Int. J. Environ. Sci. Technol.*, **2021**, *18*, 441–454. [[CrossRef](#)], [[Google Scholar](#)], [[Publisher](#)]
- [58] A.I. Obike, J.C. Igwe, C.N. Emeruwa, K.J. Uwakwe, *J. Appl. Sci. Environ. Manag.*, **2018**, *22*, 182. [[CrossRef](#)], [[Google Scholar](#)], [[Publisher](#)]
- [59] Q. Cheng, Q. Huang, S. Khan, Y. Liu, Z. Liao, G. Li, Y.S. Ok., *Ecol. Eng.*, **2016**, *87*, 240–245. [[CrossRef](#)], [[Google Scholar](#)], [[Publisher](#)]
- [60] M. Imran, M. Suddique, G. M. Shah, I. Ahmad, B. Murtaza, N. S. Shah, M. Mubeen, S. Ahmad, A. Zakir, R. J. Schotting, *Int. J. Environ. Sci. Technol.*, **2019**, *16*, 3099–3108. [[CrossRef](#)], [[Google Scholar](#)], [[Publisher](#)]
- [61] J. Chwastowski, D. Bradło, W. Żukowski, *Materials*, **2020**, *13*, 2782. [[CrossRef](#)], [[Google Scholar](#)], [[Publisher](#)]

#### HOW TO CITE THIS ARTICLE

Khaled M. Elsherif \*, Rima A. A. Saad, Abdunaser M. Ewlad-Ahmed, Abdullah A. Treban, Abdulrhman M. Iqneebir. Adsorption of Cd(II) onto Olive Stones Powder Biosorbent: Isotherms and Kinetic Studies. *Adv. J. Chem. A*, 2024, 7(1), 59-74.

DOI: [10.48309/AJCA.2024.415865.1415](https://doi.org/10.48309/AJCA.2024.415865.1415)

URL: [https://www.ajchem-a.com/article\\_182144.html](https://www.ajchem-a.com/article_182144.html)